Biochemistry & Analytical Biochemistry
ISSN: 2161-1009

Chereddy et al., Biochem Anal Biochem 2013, 2:1
DOI: 10.4172/2161-1009.1000126

Research Article Open Access

A Photoinduced Electron Transfer Based Chemosensor for the Selective Detection of Zn^{2+} Ions

Narendra Reddy Chereddy[1], Sathiah Thennarasu[1]* and Asit Baran Mandal[2]*

[1]*Organic Chemistry Division, CSIR-Central Leather Research Institute, Adyar, Chennai-600 020, India*
[2]*Chemical Laboratory, CSIR-Central Leather Research Institute, Adyar, Chennai-600 020, India*

Abstract

Aim: The chemosensors permitting naked eye detection of toxic metal ions are user-friendly, portable and obviate the requirement of sophisticated equipments. The objective of the present study was to develop a PET (Photoinduced Electron Transfer) based chemosensor for Zn^{2+} that changes its color upon binding to Zn^{2+} allowing naked eye detection.

Methods: A new 4-piperazino-1,8-naphthalimide based fluorescent probe 1 was synthesized and its structure was determined using NMR and XRD techniques. The solvatochromic effects on the absorbance and fluorescence characteristics of 1 in aqueous and non-aqueous media were explored. Metal ion competition experiements were performed to monitor the interference of common ions like Li^{+}, Na^{+}, K^{+}, Cu^{2+}, Mg^{2+}, Ca^{2+}, $Cr3^{+}$, Mn^{2+}, Fe^{2+}, Co^{2+}, Ni^{2+}, Zn^{2+}, Cd^{2+}, Hg^{2+} and Pb^{2+}.

Results and conclusion: The significance of the solvatochromic effect in colorimetric and fluorometric detection of Zn^{2+}, and turn-off sensing of Cu^{2+} via metal ion displacement have been emphasized. In non-aqueous environment, probe 1 acts as a turn-on chemosensor for Zn^{2+} and as a turn-off chemosensor towards Cu^{2+} and thereby, enables the detection of Zn^{2+} and Cu^{2+} ions in two different modes. In aqueous environment, the probe 1 acts only as a turn-off chemosensor for Cu^{2+} ion.

Keywords: Chemosensor; Naked eye detection; Solvatochromic effect; Photoinduced electron transfer

Introduction

Zinc, following iron, is the second most abundant transition metal in humans. About 2-3 g of zinc is present in an adult human body [1]. Zinc (II) ions play several roles in biological processes such as enzyme regulators, DNA binding or recognition motifs, catalytic centres and neural signal transmission [2]. The most important role for zinc is as a structural cofactor in metalloproteins [3]. The disruption of zinc pools, located primarily in muscle and bone [4] can lead to a number of diseases such as type I and type II diabetes [5,6], neural malfunction [7] particularly Alzheimer's disease [8] and certain cancers [9]. Zinc is now recognized as an important factor in the regulation of apoptosis [10]. Hence, design and synthesis of new chemosensors for the selective determination of zinc in trace levels is attaining importance. Moreover, the d^{10} electronic configuration [10] of Zn (II) makes it inactive and forbids UV-Vis spectroscopic determination. Therefore, new fluorescent indicators that show "off-on" signal in response to the presence of zinc metal ions will be advantageous in the detection and imaging of zinc sources as well as zinc contamination.

4-amino-1,8-naphthalimide is one of the most attractive fluorochromes because of its desirable properties, such as an excellent photostability, high luminescence efficiency, large Stokes shift and easy modification of the molecular structure [11,12]. Several probes for Zn^{2+} and Cu^{2+} have been reported [13-31] with 4-amino-1,8-naphthalimide as the signalling moiety, but none of them are useful for detection of both the metal ions on duel "off-on" or "on-off" modes. Generally, the fluorescence of 4-piperazino-1,8-naphthalimide derivatives is quenched due to PET arising from the piperazine nitrogen [32-35]. In the present study, binding of a Zn^{2+} ion quenches the PET process, resulting in the fluorescence emission from the chemosensor. Since the stability of metal complexes are influenced by the solvent composition, and solvent medium plays an important role on the metal ion selectivity [36-37]. It is imperative to study the effect of solvents while addressing metal ion selectivity and designing chemo sensors.

For the present study, we synthesized a 4-piperazino-1,8-naphthalimide based fluorescent probe 1 for the selective detection of Zn^{2+} ions. The solvatochromic effects of water and the routinely used non-aqueous solvent CH_3CN on the stability of 1-Zn^{2+} complex were encountered during the investigation. Interference from other competing metal ions was also investigated. The paramagnetic ion Cu^{2+} quenched the fluorescence of 1 as expected, even though Cu^{2+}-induced enhancement in fluorescence emission were observed with rhodamine based chemosensors [37-39]. The effect of the routinely used solvents water and acetonitrile on the selective detection of Zn^{2+} and Cu^{2+} ions, and the mechanistic aspects involved in complex formation were explored.

Experimental Section

General

Dry acetonitrile and double distilled water were used in all experiments. All the materials for synthesis were purchased from commercial suppliers and used without further purification. The

***Corresponding author:** Sathiah Thennarasu, Organic Chemistry Division, CSIR-Central Leather Research Institute, Adyar, Chennai-600 020, India, Tel: +91 44 24913289; Fax: +91 44 24911589; E-mail: thennarasu@gmail.com

Asit Baran Mandal, Chemical Laboratory, CSIR-Central Leather Research Institute, Adyar, Chennai-600 020, India, E-mail: abmandal@hotmail.com

Received January 16, 2013; **Accepted** February 11, 2013; **Published** February 15, 2013

Citation: Chereddy NR, Thennarasu S, Mandal AB (2013) A Photoinduced Electron Transfer Based Chemosensor for the Selective Detection of Zn^{2+} Ions. Biochem Anal Biochem 1:126. doi:10.4172/2161-1009.1000126

solutions of metal ions were prepared from the corresponding chloride salts. Absorption spectra were recorded on a SPECORD 200 PLUS UV-Visible spectrophotometer. Fluorescence measurements were performed on a Cary Eclipse fluorescence spectrophotometer. NMR spectra were recorded using a JEOL-ECP500 MHz spectrometer operated at 500 MHz. ESI-MS spectra were obtained on a Thermo Finnigan LCQ Advantage MAX 6000 ESI spectrometer. Absorption and fluorescence measurements were made using a 3.0 mL cuvette.

Synthesis of bromoacetylamino quinoline (o)

The bromoacetylamino quinoline was synthesized in a single-step procedure. To a mixture of 8-aminoquinoline (0.72 g, 5.0 mmol) and triethylamine (0.60 g, 6.0 mmol) in dichloromethane (DCM) (20 mL) at 0°C, bromoacetylbromide (1.21 g, 6.0 mmol) was added drop-wise, and the reaction mixture was stirred at room temperature for 3 h. The progress of the reaction was monitored using TLC. After completion, the reaction mixture was washed with water and subjected to column chromatography (silica gel 100-200 mesh) and eluted using hexane-ethtyl acetate (98:2) mixture to get 1.06 g (80%) of bromoacetylamino quinoline (B) in pure form as pale yellow solid.

Synthesis of naphthalimide derivative 1

To a solution of 4-bromo-1,8-naphthanoic anhydride (1.0 g, 3.6 mmol) in EtOH maintained at 80°C, propylamine (1.0 mL) was added slowly. The resulting mixture was stirred for 1h and cooled to room temperature. The precipitate formed was filtered and used in the next step. To this product, 4-bromo-N-propyl-1,8-naphthanamide, (0.7 g, 2.2 mmol) in DMSO, piperazine (1.00 g, 11.6 mmol) and K_2CO_3 (0.42 g, 3.0 mmol) were added and stirred at 120°C for 3h. After completion of the reaction, the mixture was extracted with DCM, concentrated and subjected to column chromatography (silica gel 100-200 mesh) and eluted using ethyl acetate to get 0.50 g (70%) of 4-piperazinyl-N-propyl-1,8-naphthalimide (p). In order to prepare the desired compound 1, 4-piperazinyl-N-propyl-1,8-naphthalimide (p) (0.32 g, 1.0 mmol) and K_2CO_3 (0.14 g, 1.0 mmol) were dissolved in DMF. To the resultant mixture, bromoacetylamino quinoline (o) (0.30 g, 1.1 mmol) was added and stirred at room temperature overnight. After completion of the reaction, the mixture was extracted with DCM, concentrated and subjected to column chromatography (silica gel 100-200 mesh) and eluted using hexane-ethtyl acetate (80:20) mixture to get 0.40 g (80%) of probe 1 as yellow solid.

NMR and mass data of napthalimide derivative 1

$^{1]}$H NMR ($CDCl_3$, 500 MHz), δ (ppm): 1.02 (t, *J*=7.6 Hz, 3H, $NCH_2CH_2CH_3$), 1.78 (m, 2H, $NCH_2CH_2CH_3$), 3.05 (s, 4H, Piperazine-CH_2), 3.51 (d, 2H, N-CH_2-C=O), 3.49 (m, 4H, Piperazine-CH_2), 4.15 (t, 2H, $NCH_2CH_2CH_3$), 7.31(d, *J* = 8.0 Hz, 1H, Ar-H), 7.46 (m, 1H, Ar-H), 7.55 (m, 2H, Ar-H), 7.71 (t, *J*=8.0 Hz, 1H, Ar-H), 8.17 (dd, *J*=1.5 Hz, 1H, Ar-H), 8.44 (d, *J*=8.0 Hz, 1H, Ar-H) 8.58 (m, 2H, Ar-H), 8.79 (dd, *J*=1.5 Hz, 1H, Ar-H) 8.85 (dd, *J*=1.0 Hz, 1H, Ar-H), 11.49 (s, 1H, Amide-NH). ^{13}C NMR ($CDCl_3$, 100 MHz), δ (ppm): 11.66, 21.53, 41.90, 53.43,53.59, 62.49, 115.07, 116.73, 117.10, 121.73, 121.99, 123.42, 125.91, 126.28, 129.97, 130.25, 131.25, 132.57, 134.26, 136.37, 139.08, 148.70, 155.86, 164.15, 164.57,168.75. ESI-MS: calcd for $C_{30}H_{29}N_5O_3$ m/z (M^+) 507.2, found $(M+H)^+$ 508.3.

Results and Discussion

Synthesis and structure determination of probe 1

The 4-piperazino-1,8-naphthalimide based fluorescent probe 1 was synthesized in four convenient steps as outlined in figure 1 and characterized using NMR (Figure S1-S2, ESI), ESI-Mass (Figure S3, ESI), and single crystal X-ray crystallographic techniques (Figure 2, CCDC 888111). The proton NMR spectrum of 1 in $CDCl_3$ displayed a triplet at 1.02 ppm, a triplet 4.15 ppm and a multiplet at 1.78 ppm arising from the propyl group attached to the naphthalimide moiety. The two broad peaks at 3.48 and 3.05 ppm were assigned to the two types of methylene protons on the piperazine moiety. The presence of a doublet at 3.51 ppm corresponding to the linker moiety (N-CH_2-C=O) confirms the attachment of 8-aminoquinoline to the 4-piperazino-1,8-naphthalimide derivative. The signals seen in the ^{13}C NMR spectrum are in good agreement with the proposed structure. ESI-Mass analysis of the probe 1 also supports the proposed structure. Finally, X-ray diffraction analysis of single crystals of the probe 1 confirmed the three dimensional structure (Figure 2).

Metal ion selectivity and sensitivity of probe 1

The fluorescence of 4-piperazino-1,8-naphthalimide derivatives are usually quenched either completely or partially due to PET [32-35]. During our screening experiments involving different solvents and metal ions, probe 1 showed significant quantum of fluorescence in aqueous and non-aqueous media indicating partial quenching due to PET process. The fluorescence emission intensity of probe 1 in neat CH_3CN was decreased upon addition of incremental quantities of water, indicating the ability of water to interfere with the life time of the excited state of probe 1, presumably, facilitating the non-radioactive decay. Hence, we investigated the probe's ability for the detection of different metal ions in aqueous and non-aqueous media.

A 10 μM solution of probe 1 in CH_3CN emits green fluorescence, as shown in figure 3. Addition of various metal ions (50 μM) like Li^+, Na^+, K^+, Mg^{2+}, Ca^{2+}, $Cr3^+$, Mn^{2+}, $Fe3^+$, Co^{2+}, Ni^{2+}, Cd^{2+}, Hg^{2+} or Pb^{2+} does not

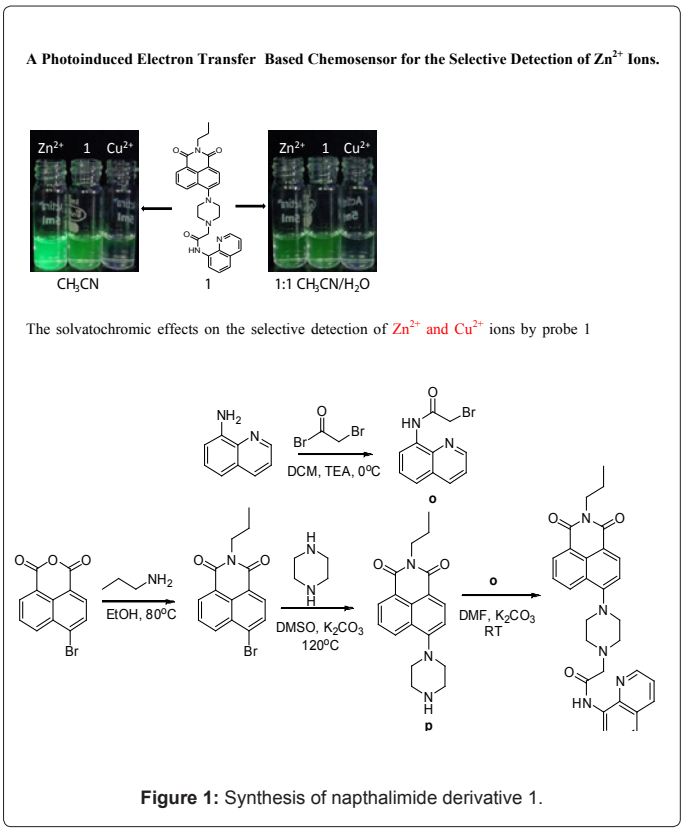

Figure 1: Synthesis of napthalimide derivative 1.

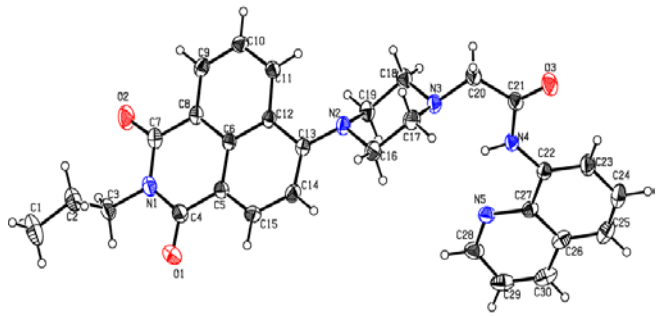

Figure 2: ORTEP diagram of probe 1.

change either the colour or the fluorescence intensity of the solution. Interestingly, addition of 50 μM Zn^{2+} produces a distinct colour change due to fluorescence enhancement, while 50 μM Cu^{2+} turns off the fluorescence signal. This dual performance of probe 1 enables the naked-eye detection of both Zn^{2+} and Cu^{2+} ions in 'On' and 'Off' modes, respectively (Figure 3a). However, when the solvent system is changed from CH_3CN to CH_3CN/H_2O (1:1) mixture, the probe 1 fails to discriminate Zn^{2+} from other metal ions while retaining the 'Off' signal for Cu^{2+} (Figure 3b). It appears, therefore, that the high polarity of aqueous CH_3CN (1:1 CH_3CN/H_2O) medium effectively nullifies the Zn^{2+}-induced enhancement in the fluorescence of 1, and thereby, permits only Cu^{2+} selective 'turn-off' sensing.

Influence of solvent on Zn^{2+} and Cu^{2+} complex formation

The absorbance characteristics of probe 1 (10 μM) in CH_3CN and CH_3CN/H_2O (1:1) mixture containing equimolar quantities of different metal ions are shown in figure 4. In neat CH_3CN, probe 1 exhibits two absorbance maxima, one corresponding to quinoline moiety (~242 nm) and the other arising from naphthalimide moiety (~408 nm). Addition of various metal ions (10 μM), excepting Zn^{2+} and Cu^{2+}, does not induce any changes in the absorption pattern of 1 (Figure 4a). The addition of Zn^{2+} (10 μM) causes a red shift in the absorbance maximum of quinoline moiety (from ~242 to ~255 nm). However, no significant changes are observed in the absorbance maximum of naphthalimide moiety (Figure 4a). This marked red shift in the absorbance maximum of quinoline moiety and the absence of any significant changes in the absorbance maximum of naphthalimide moiety clearly indicate that Zn^{2+} is bound to the probe 1, but not to the piperazine 'N' attached to the naphthalimide moiety. A similar titration in CH_3CN/H_2O (1:1) mixture (Figure 4b) shows the absence of any red shift in the absorbance maximum of quinoline moiety, and indicates the destabilizing effect of water in the formation and stability of 1-Zn^{2+} complex.

A similar study with Cu^{2+} provides a different picture of the destabilizing effect of water on the stability of 1-Cu^{2+} complex (Figures 4a and 4b). The addition of Cu^{2+} (10 μM) shifts the absorbance maximum of quinoline moiety (red shift: from ~242 to ~255 nm) and that of naphthalimide moiety (blue shift: from ~408 to ~399 nm) in neat CH_3CN. The blue shift is more pronounced in CH_3CN/H_2O (1:1) mixture (from ~399 to ~389 nm). These shifts in absorbance clearly indicate that Cu^{2+} is bound to the piperazine 'N' attached to the naphthalimide moiety, and thereby, decreases the electron donating capacity of the latter in both the solvents.

The variations in the absorbance pattern of probe 1 (10 μM) in neat CH_3CN, in response to the addition of serial concentrations of Zn^{2+} and Cu^{2+} are shown in figure 5. In both the cases, the absorbance at

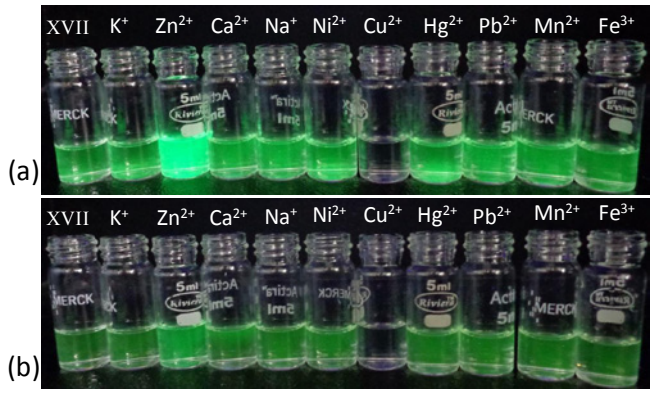

Figure 3: Effect of addition of various metal ions (50 μM) to 10 μM solution of probe 1 in (a) CH_3CN and (b) 1:1 CH_3CN/H_2O.

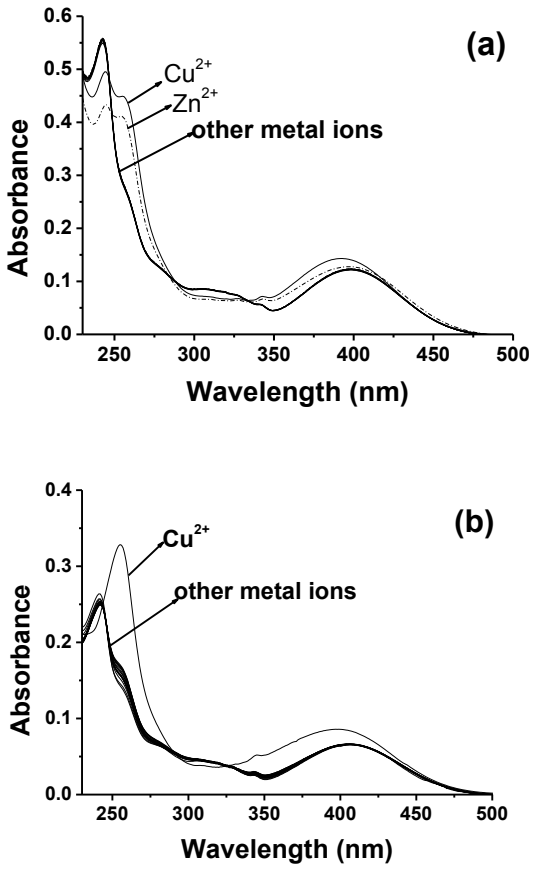

Figure 4: Metal ion (10 μM) induced variations in the absorbance spectra of 1 (10 μM) in (a) CH_3CN and (b) 1:1 CH_3CN/H_2O.

~255 nm reached the maximum at 20 μM concentrations of metal ions. However, the incremental increase in the peak intensity at ~255 nm is more pronounced on the addition of Cu^{2+} ions (Figure 5b) than on the addition of Zn^{2+} ions (Figure 5a). This observation sheds light on the relative stabilities of the respective complexes formed.

In a similar experiment carried out in 1:1 CH_3CN/H_2O medium, significant variations in the absorbance of probe 1 (10 μM) are observed only upon addition of serial concentrations of Cu^{2+} ions. Upon addition

of one equivalent of Cu^{2+}, the absorbance maximum at ~255 nm reaches the maximum level (Figure 6b) suggesting the formation of a 1:1 complex with probe 1. Such a complex formation with Zn^{2+} is not observed even after the addition of 30 μM Zn^{2+} ions as indicated by the absence of the red shifted peaks at ~255 nm arising from the absorbance maximum of quinoline moiety (Figure 6a).

Solvent assisted dual mode sensing of Zn^{2+} and Cu^{2+}

Since the fluorescence of probe 1 is quenched by water, all fluorescence measurements were carried out in 100% CH_3CN for dual detection of Zn^{2+} and Cu^{2+} ions. The effect of different metal ions on the fluorescence emission intensity of probe 1 (10 μM) is shown in figure 7a. Whereas the addition of Zn^{2+} (10 μM) enhances the fluorescence to a significant level, the addition of Cu^{2+} (10 μM) quenches the fluorescence emission intensity almost completely. Confirmation of the opposing contributions of Zn^{2+} and Cu^{2+} is seen in the fluorescence spectra of 1 in the presence of serial concentrations of Zn^{2+} and Cu^{2+} ions (Figures 7b and 7c). Other common metal ions do not affect the fluorescence emission spectrum of probe 1. These results reveal that probe 1 could be used to detect Zn^{2+} and Cu^{2+} from normally co-existing metal ions, albeit, at two different modes.

The metal ion competition experiments exemplifies that Zn^{2+} (10 μM) induced fluorescence enhancement of probe 1 is unaffected by even five-fold excess amounts of other metal ions like Li^{+}, Na^{+}, K^{+}, Mg^{2+}, Ca^{2+}, $Cr3^{+}$, Mn^{2+}, $Fe3^{+}$, Co^{2+}, Ni^{2+}, Cd^{2+}, Hg^{2+} and Pb^{2+}. However, complete quenching of fluorescence is observed by the addition of an equimolar quantity of Cu^{2+}, indicating the higher binding affinity for

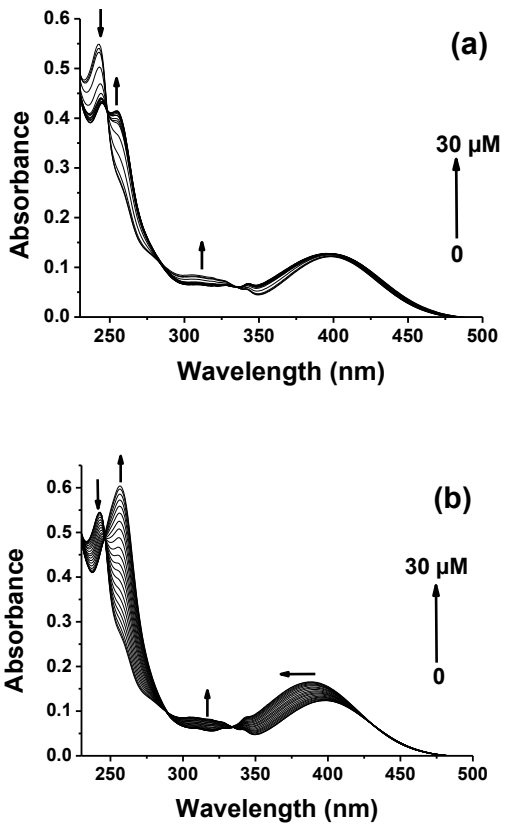

Figure 5: Metal ion dependent variations in the absorbance of probe 1 (10 μM) in CH_3CN: (a) Zn^{2+} concentration is 0-30 μM and (b) Cu^{2+} concentration is 0-30 μM.

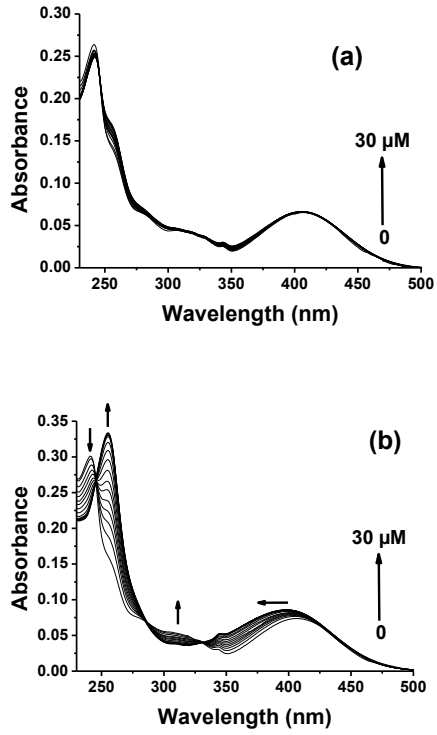

Figure 6: Metal ion dependent variations in the absorbance of probe 1 (10 μM) in 1:1 CH_3CN/H_2O: (a) Zn^{2+} concentration is 0-30 μM and (b) Cu^{2+} concentration is 0-30 μM.

Cu^{2+} as compared to Zn^{2+} (Figure S4, ESI). The higher binding affinity of probe 1 for Cu^{2+} over Zn^{2+} is confirmed by the binding constants calculated [40] for 1-Cu^{2+} (5.8×10^{5} M^{-1}) and 1-Zn^{2+} (3×10^{5} M^{-1}) complexes. Further, addition of Cu^{2+} (10 μM) to probe 1 equilibrated with the other metal ions (50 μM) also results in complete quenching of fluorescence (Figure S5, ESI).

It appears, therefore, that upon addition of Cu^{2+} to the fluorescent 1-Zn^{2+} complex, Cu^{2+} replaces Zn^{2+} in the complex leading to the formation of a non-fluorescent 1-Cu^{2+} complex (Figure 8). Moreover, addition of EDTA to 1-Cu^{2+} complex restores the fluorescence characteristics of probe 1. This indicates that the formation of 1-Zn^{2+} and 1-Cu^{2+} complexes is reversible and that the changes in the fluorescence characteristics of probe 1 in response to the addition of Zn^{2+} and Cu^{2+} ions are due to complex formation (Figure S6, ESI) and not due to any catalytic action.

Thus, the UV-Visible and fluorescence experiments clearly establish Zn^{2+} induced red shift of the absorbance of quinoline moiety in probe 1. This red shift in the absorbance could be attributed to the change in the electronic delocalization of the quinoline moiety upon Zn^{2+} binding. Further insight into the reason as to why these changes occur in the absorption and fluorescence emission upon addition of Zn^{2+}, could be gained using NMR and ESI-MS techniques.

Binding sites for Zn^{2+} and Cu^{2+} on probe 1 are different

Analysis of the ^{1}H-NMR spectra of the probe 1 alone, and in the presence of serial concentrations of Zn^{2+} (Figure S7, ESI) clearly show that the piperazine protons labelled as 'a' in figure 9, shift to down field, and that the intensity of the amide proton decreases while the intensity of the other protons remain unchanged. The deshielding effect

experienced by the piperazine protons labelled as 'a' is not observed with the piperazine protons labelled as 'b' in figure 9.

The ^{13}C-NMR spectra recorded under identical conditions (Figure S8, ESI) show the disappearance of the amide carbonyl resonance at ~170 ppm, indicating its involvement in complex formation. Taken together, the NMR data confirm the involvement of the piperazine 'N' and carbonyl 'O', in 1-Zn^{2+} complex formation and the induction of extended conjugation with the quinoline moiety. This also explains the red shift in the absorbance maximum of quinoline moiety upon 1-Zn^{2+} complex formation. Since the piperazine 'N' has the ability to quench the fluorescence of the naphalimide moiety by PET process, the 1-Zn^{2+} complex formation would decrease the electron density at piperazine 'N', reduce the effect of PET process on napthalimide moiety, and thereby, enhance the fluorescence intensity. This proposition is further supported by ESI-MS spectrum (Figure S6, ESI). The ESI-MS spectrum of 1-Zn^{2+} complex also confirms the 2:1 ligand:metal geometry of the fluorescent complex with subsequent deprotonation of amide 'NH' as shown in figure 9. Further, addition of Cu^{2+} to the fluorescent 1-Zn^{2+} complex, leads to the formation of a non-fluorescent 1-Cu^{2+} complex via metal ion displacement (Figure 8).

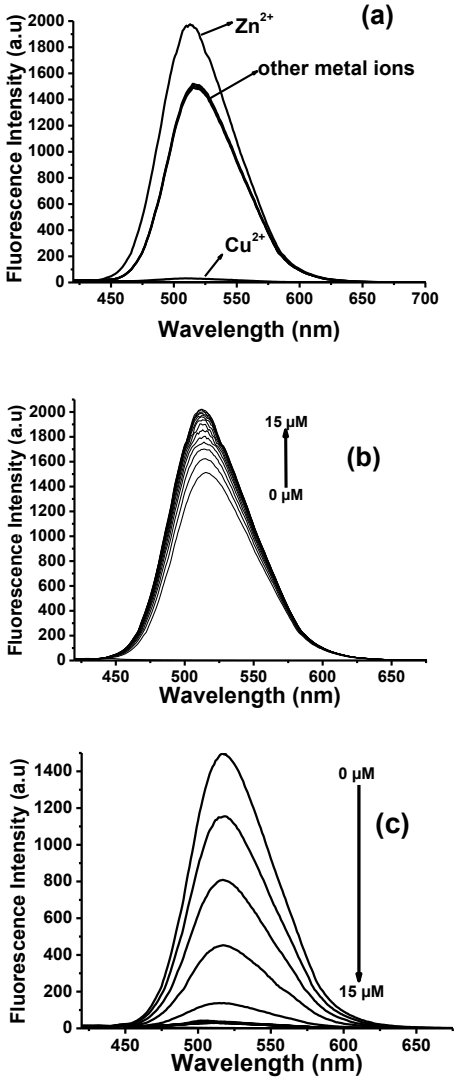

Figure 7: Variations in the fluorescence spectra of 1 (10 μM) in CH_3CN induced by (a) common metal ions (10 μM), (b) Zn^{2+} ions at indicated concentrations, and (c) Cu_{2+} ions at indicated concentrations.

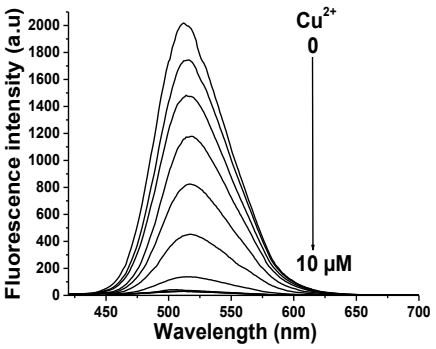

Figure 8: Effect of addition of Cu_{2+} on the fluorescence emission of 1-Zn_{2+} complex.

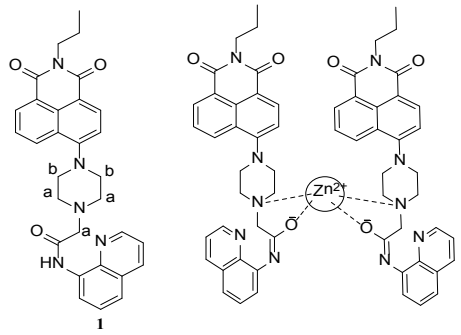

Figure 9: The perspective Zn^{2+} binding pattern with probe 1.

Conclusion

The synthesis, structure determination and physicochemical properties of a chemosensor that emits fluorescence only upon complex formation with Zn^{2+}, are described. Probe 1 selectively detects Cu^{2+} in aqueous environment by fluorescence "on-off" mechanism. In non-aqueous medium, it acts as a dual sensor for Zn^{2+} and Cu^{2+}, albeit, in two different modes. The mechanistic aspects involved in metal ion detection are demonstrated. Water plays a significant role in colorimetric and fluorometric detection as well as metal-ligand complex formation. The observations of this study emphasize the importance of solvent screening during the development of new fluorescent probes for the selective detection of specific metal ions.

References

1. Cotton FA, Wilkinson G (1988) Advanced Inorganic Chemistry. (5thedn), Wiley.
2. Berg JM, Shi Y (1996) The galvanization of biology: a growing appreciation for the roles of zinc. Science 271: 1081-1085.
3. Auld DS (2001) Zinc coordination sphere in biochemical zinc sites. Biometals 14: 271-313.
4. Hambidge KM, Casey CE, Krebs NF (1986) Zinc. In: Trace Elements in Human and Animal Nutrition (5th edn), Academic Press, Orlando, FL.
5. Sladek R, Rocheleau G, Rung J, Dina C, Shen L, et al. (2007) A genome-wide association study identifies novel risk loci for type 2 diabetes. Nature 445: 881-885.
6. Chimienti F, Devergnas S, Pattou F, Schuit F, Garcia-Cuenca R, et al. (2006) *In*

vivo expression and functional characterization of the zinc transporter ZnT8 in glucose-induced insulin secretion. J Cell Sci 119: 4199-4206.

7. Que EL, Domaille DW, Chang CJ (2008) Metals in neurobiology: probing their chemistry and biology with molecular imaging. Chem Rev 108: 1517-1549.
8. Frederickson CJ, Koh JY, Bush AI (2005) The neurobiology of zinc in health and disease. Nat Rev Neurosci 6: 449-462.
9. Costello LC, Franklin RB, Feng P, Tan M, Bagasra O (2005) Zinc and prostate cancer: a critical scientific, medical, and public interest issue (United States). Cancer Causes Control 16: 901-915.
10. Zalewski PD, Forbes IJ, Betts WH (1993) Correlation of apoptosis with change in intracellular labile Zn(II) using zinquin [(2-methyl-8-p-toluenesulphonamido-6-quinolyloxy)acetic acid], a new specific fluorescent probe for Zn(II). Biochem J 296: 403-408.
11. Gunnlaugsson T, Kruger PE, Lee TC, Parkesh R, Pfeffe FM, et al. (2003) Biomimetic syntheses of stizolobic acid and 3-(6-carboxy-2-oxo-4-pyridyl) alanine. Tetrahedron Lett 35: 6575-6576.
12. Gunnlaugsson T, Kruger PE, Jensen P, Tierney J, Ali HD, et al. (2005) Colorimetric "naked eye" sensing of anions in aqueous solution. J Org Chem 70: 10875-10878.
13. Wang H, Yang L, Zhang W, Zhou Y, Zhao B, et al. (2012) A colorimetric probe for copper(II) ion based on 4-amino-1,8-naphthalimide. Inorganica Chim Acta 381: 111-116.
14. Jisha VS, Thomas AJ, Ramaiah D (2009) Fluorescence ratiometric selective recognition of Cu(2+) ions by dansyl-naphthalimide dyads. J Org Chem 74: 6667-6673.
15. Shankar BH, Ramaiah D (2011) Dansyl-naphthalimide dyads as molecular probes: effect of spacer group on metal ion binding properties. J Phys Chem B 115: 13292-13299.
16. Xu Z, Qian X, Cui J (2005) Colorimetric and Ratiometric Fluorescent Chemosensor with a Large Red-Shift in Emission: Cu(II)-Only Sensing by Deprotonation of Secondary Amines as Receptor Conjugated to Naphthalimide Fluorophore. Org lett 7: 3029-3032.
17. Mu H, Gong R, Ma Q, Sun Y, Fu E (2007) A novel colorimetric and fluorescent chemosensor: synthesis and selective detection for Cu^{2+} and Hg^{2+}. Tetrahedron Lett 48: 5525-5529.
18. Singh N, Kaur N, McCaughan B, Callan JF (2010) Ratiometric fluorescent detection of Cu(II) in semi-aqueous solution using a two-fluorophore approach. Tetrahedron Lett 51: 3385-3387.
19. Goswami S, Sen D, Das NK, Hazra G (2010) Highly selective colorimetric fluorescence sensor for Cu^{2+}: cation-induced 'switching on' of fluorescence due to excited state internal charge transfer in the red/near-infrared region of emission spectra. Tetrahedron Lett 51: 5563-5566.
20. Yang H, Song H, Zhu Y, Yang S (2012) Single chemosensor for multiple analytes: chromogenic and fluorogenic detection for fluoride anions and copper ions. Tetrahedron Lett 53: 2026-2029.
21. Tamanini E, Katewa A, Sedger LM, Todd MH, Watkinson M (2009) A synthetically simple, click-generated cyclam-based zinc(II) sensor. Inorg Chem 48: 319-324.
22. Tamanini E, Flavin K, Motevalli M, Piperno S, Gheber LA, et al. (2010) Cyclam-based "clickates": homogeneous and heterogeneous fluorescent sensors for Zn(II). Inorg Chem 49: 3789-3800.
23. Zhang LJ, Chen HL, Li ZF, Lu ZL, Wang R (2012) Click-reaction generated [12]aneN_3-based fluorescent sensor for Zn(II) ions. Inorg Chem Commun 23: 67-69.
24. Xu Z, Baek KH, Kim HN, Cui J, Qian X, et al. (2010) Zn^{2+}-triggered amide tautomerization produces a highly Zn^{2+}-selective, cell-permeable, and ratiometric fluorescent sensor. J Am Chem Soc 132: 601-610.
25. Wang J, Xiao Y, Zhang Z, Qian X, Yanga Y, et al. (2005) A pH-resistant Zn(II) sensor derived from 4-aminonaphthalimide: design, synthesis and intracellular applications. J Mater Chem 15: 2836-2839.
26. Lu C, Xu Z, Cui J, Zhang R, Qian X (2007) Ratiometric and highly selective fluorescent sensor for cadmium under physiological pH range: a new strategy to discriminate cadmium from zinc. J Org Chem 72: 3554-3557.
27. Parkesh R, Clive Lee T, Gunnlaugsson T (2007) Highly selective 4-amino-1,8-naphthalimide based fluorescent photoinduced electron transfer (PET) chemosensors for Zn(II) under physiological pH conditions. Org Biomol Chem 5: 310-317.
28. Gunnlaugsson T, Lee TC, Parkesh R (2003) A highly selective and sensitive fluorescent PET (photoinduced electron transfer) chemosensor for Zn(II). Org Biomol Chem 1: 3265-3267.
29. Lee S, Lee JH, Pradhan T, Lim CS, Cho BR, et al. (2011) Fluorescent turn-on Zn^{2+} sensing in aqueous and cellular media. Sens Actuators B Chem 160: 1489-1493.
30. Xu Z, Qian X, Cuia J, Zhang R (2006) Exploiting the deprotonation mechanism for the design of ratiometric and colorimetric Zn^{2+} fluorescent chemosensor with a large red-shift in emission. Tetrahedron 62: 10117-10122.
31. Kim SY, Hong JI (2009) Naphthalimide-based fluorescent Zn^{2+} chemosensors showing PET effect according to their linker length in water. Tetrahedron Lett 50: 2822-2824.
32. Li CY, Zhou Y, Xu F, Li YF, Zou CX, et al. (2012) A fluorescent pH chemosensor based on functionalized naphthalimide in aqueous solution. Anal Sci 28: 743-747.
33. Tian Y, Su F, Weber W, Nandakumar V, Shumway BR, et al. (2010) A series of naphthalimide derivatives as intra and extracellular pH sensors. Biomaterials 31: 7411-7422.
34. Gan J, Chen K, Chang CP, Tian H (2003) Luminescent properties and photo-induced electron transfer of naphthalimides with piperazine substituent. Dyes Pigm 57: 21-28.
35. Bojinov VB, Georgiev NI, Bosch P (2009) Design and synthesis of highly photostable yellow-green emitting 1,8-naphthalimides as fluorescent sensors for metal cations and protons. J Fluoresc 19: 127-139.
36. Hao E, Meng T, Zhang M, Pang W, Zhou Y, et al. (2011) Solvent Dependent Fluorescent Properties of a 1,2,3-Triazole Linked 8-Hydroxyquinoline Chemosensor: Tunable Detection from Zinc(II) to Iron(III) in the CH_3CN/H_2O System. J Phys Chem A 115: 8234-8241.
37. Chereddy NR, Janakipriya S, Korrapati PS, Thennarasu S, Mandal AB (2013) Solvent-assisted selective detection of sub-micromolar levels of Cu(2+) ions in aqueous samples and live-cells. Analyst 138: 1130-1136.
38. Chereddy NR, Thennarasu S (2011) Synthesis of a highly selective bis-rhodamine chemosensor for naked-eye detection of Cu^{2+} ions and its application in bio-imaging. Dyes Pigm 91: 378-382.
39. Chereddy NR, Thennarasu S, Mandal AB (2012) A new triazole appended rhodamine chemosensor for selective detection of Cu^{2+} ions and live-cell imaging. Sens Actuators B Chem.
40. Tedesco AC, Oliveira DM, Lacava ZGM, Azevedo RB, Lima ECD, et al. (2004) Investigation of the binding constant and stoichiometry of biocompatible cobalt ferrite-based magnetic fluids to serum albumin. J Magn Magn Mater 272-276: 2404-2405.

Citation: Chereddy NR, Thennarasu S, Mandal AB (2013) A Photoinduced Electron Transfer Based Chemosensor for the Selective Detection of Zn^{2+} Ions. Biochem Anal Biochem 1:126. doi:10.4172/2161-1009.1000126